

Elastic properties of single-walled carbon nanotubes

V. N. Popov* and V. E. Van Doren

Physics Department, University of Antwerp (RUCA), Groenenborgerlaan 171, B-2020 Antwerp, Belgium

M. Balkanski

Université Pierre et Marie Curie, 4 Place Jussieu, F-75252 Paris Cedex 05, France

(Received 6 July 1999; revised manuscript received 22 September 1999)

Analytical expressions for the velocities of the longitudinal and the torsional sound waves in single-walled carbon nanotubes are derived using Born's perturbation technique within a lattice-dynamical model. These expressions are compared to the formulas for the velocities of the sound waves in an elastic hollow cylinder from the theory of elasticity to obtain analytical expressions for the Young's and shear moduli of nanotubes. The calculated elastic moduli for different chiral and achiral (armchair and zigzag) nanotubes using force constants of the valence force field type are compared to the existing experimental and theoretical data.

I. INTRODUCTION

Since the discovery of the multiwalled carbon nanotubes (MWNT's) in the soot produced by the arc discharge technique^{1,2} much attention has been given to the investigation of their amazing physical properties.³ Recently, the mass production of single-walled carbon nanotubes (SWNT's), stacked in crystalline ropes, was made possible by the laser ablation⁴ and by the arc discharge⁵ techniques. Due to their specific structure, the nanotubes are expected to be as stiff as graphite along the graphene layers or even reach the stiffness of diamond. This unique mechanical property of the nanotubes combined with their light-weightness predetermines their usage in composite materials and has motivated precise experimental measurements of their elastic properties.⁶⁻⁹ In the first of these works,⁶ the temperature dependence of the vibration amplitude of several isolated MWNT's was analyzed in a transmission electron microscope to eventually obtain 1.8 TPa for the average Young's modulus. Later on, this technique was applied to measure Young's modulus of isolated SWNT's in the diameter range 1.0–1.5 nm and an average value $\langle Y \rangle = 1.25 - 0.35 / + 0.45$ TPa was derived.⁷ In another experimental approach⁸ the MWNT's were pinned to a substrate by conventional lithography and the force was measured at different distances from the pinned point by atomic force microscope (ATM). The average Young's modulus for different MWNT's with diameters from 26 to 76 nm was found to be 1.28 ± 0.59 TPa. Recently, Young's and shear moduli of ropes of SWNT's were measured by suspending the ropes over the pores of a membrane and using ATM to determine directly the resulting deflection of the rope.⁹ The theoretical estimation of the elastic moduli was accomplished exclusively by numerical second derivatives of the energy of the strained nanotubes. In the calculation of the elastic moduli of various SWNT's within a simple force-constant model¹⁰ it was found that the moduli were insensitive to tube size and helicity and had the average values of $\langle Y \rangle = 0.97$ TPa and $\langle G \rangle = 0.45$ TPa. In several works, molecular-dynamics (MD) simulation algorithms using the Tersoff-Brenner potential for the carbon-carbon interactions were implemented to relax the strained nanotubes and calculate their energy.¹¹⁻¹³ For tubes of diameter of 1 nm values for Y of 5.5 TPa (Ref. 12) and 0.8 TPa (Ref. 13) were ob-

tained. A non-orthogonal tight-binding (TB) scheme was applied to calculate Young's modulus of several chiral and achiral SWNT's yielding an average value of 1.24 TPa.¹⁴ Recently, the second derivative of the strain energy with respect to the axial strain, calculated with a pseudopotential density-functional-theory (DFT) model for a number of SWNT's,¹⁵ was found to vary slightly with the tube type and to have the average value of 56 eV.

In this paper, we choose a different approach to the calculation of the elastic properties of SWNT's. Namely, we derive analytical expressions for the elastic (Young's and shear) moduli of SWNT's using a perturbation technique due to Born¹⁶ within a lattice-dynamical model for nanotubes.¹⁷ This scheme has the advantage that the elastic moduli are consistent with the lattice dynamics of the nanotubes and that each of these moduli is obtained in one calculational step only.

The essential features of a model of the lattice dynamics of SWNT's based on the explicit accounting for the helical symmetry of the tubes¹⁷ are summarized in Sec. II A. This model is applied to study of the long-wavelength vibrations in nanotubes using Born's perturbation technique¹⁶ and to obtain analytical expressions for the velocities of the longitudinal and the torsional sound waves in SWNT's (see Sec. II B). The comparison of these expressions with the formulas from the theory of elasticity for the velocities of these waves in an elastic hollow cylinder allows one to determine the Young's and shear moduli of the nanotubes. The calculated phonon dispersion of a (10,10) nanotube and elastic moduli for various chiral and achiral (armchair and zigzag) nanotubes using force constants of the valence force field (VFF) type¹⁸ are presented in Sec. III and discussed in comparison with the existing experimental and theoretical data.

II. THEORY

A. The lattice-dynamical model

The ideal nanotube structure can be obtained from a graphene sheet by rolling it up along the straight line connecting two lattice points into a seamless cylinder in such a way that the two points coincide.^{11,19,20} The tube is uniquely

specified by the pair of integers (L_1, L_2) that define the lattice translation vector between the two points. Alternatively, the tube can be described by its radius R and the chiral angle θ that is the angle between the tube circumference and the nearest zigzag of carbon-carbon bonds. The tubes are called achiral for $\theta=0$ (zigzag type) and $\theta=\pi/6$ (armchair type), and chiral for $0<\theta<\pi/6$.

The nanotube can be considered as a crystal lattice with a two atoms unit cell. Two different screw operators can be used to construct the entire tube from these two atoms²¹ in quite the same way as a crystal is generated by means of primitive translation vectors. By definition, a screw operator $\{S_i|\mathbf{t}_i\}$ ($i=1,2$) executes a rotation of the position vector of an atom by an angle ϕ_i about the tube axis with rotation matrix S_i and a translation of this vector by a vector \mathbf{t}_i along the same axis. Thus, the equilibrium position vector $\mathbf{R}(l_1 l_2 k)$ of the k th atom in the (l_1, l_2) th cell is obtained from $\mathbf{R}(k) \equiv \mathbf{R}(00k)$ as

$$\mathbf{R}(lk) = S(l)\mathbf{R}(k) + \mathbf{t}(l), \quad (2.1)$$

where the compact notation $S(l) = S_1^{l_1} S_2^{l_2}$, $\mathbf{t}(l) = l_1 \mathbf{t}_1 + l_2 \mathbf{t}_2$, and $l = (l_1, l_2)$ is adopted.

A lattice-dynamical model for a SWNT can be constructed in a similar way as for a three-dimensional crystal.¹⁷ In particular, the equation of motion for small displacements $\mathbf{u}(lk)$ of the atoms from their equilibrium positions are given by

$$m_k \ddot{\mathbf{u}}_\alpha(lk) = - \sum_{l'k'} \Phi_{\alpha\beta}(lk, l'k') u_\beta(l'k'), \quad (2.2)$$

where m_k is the atomic mass of the k th atom and $\Phi_{\alpha\beta}(lk, l'k')$ is the force-constant matrix ($\alpha, \beta = x, y, z$). The helical symmetry of the tubes described by the two screw operators suggests to look for wavelike solutions for the atomic displacement vectors $\mathbf{u}(lk)$ of the type

$$u_\alpha(lk) = \frac{1}{\sqrt{m_k}} \sum_{\beta} S_{\alpha\beta}(l) e_\beta(k|\mathbf{q}) \exp\{i[\mathbf{q} \cdot \mathbf{l} - \omega(\mathbf{q})t]\} \quad (2.3)$$

with wave vector $\mathbf{q} = (q_1, q_2)$, wave amplitude $e_\beta(k|\mathbf{q})$ and angular frequency $\omega(\mathbf{q})$. After substituting Eq. (2.3) in Eq. (2.2), the equations of motion are obtained in the form

$$\omega^2(\mathbf{q}) e_\alpha(k|\mathbf{q}) = \sum_{k'\beta} D_{\alpha\beta}(kk'|\mathbf{q}) e_\beta(k'|\mathbf{q}), \quad (2.4)$$

where

$$D_{\alpha\beta}(kk'|\mathbf{q}) = \frac{1}{\sqrt{m_k m_{k'}}} \sum_{l'\gamma} \Phi_{\alpha\gamma}(\mathbf{0}k, l'k') S_{\gamma\beta}(l') \exp(i\mathbf{q} \cdot \mathbf{l}'). \quad (2.5)$$

is the dynamical matrix. The rotational boundary condition¹⁹⁻²¹ and the translational periodicity condition²² on $\mathbf{u}(lk)$ impose the following constraints on the wave-vector components

$$q_1 L_1 + q_2 L_2 = 2\pi l \quad (2.6)$$

and

$$q_1 N_1 + q_2 N_2 = q. \quad (2.7)$$

Here, l is an integer number, N_c is the number of atomic pairs in the translational unit cell of the tube, q is a new, one-dimensional wave vector, and the integers N_1 and N_2 define the primitive translation vector of the tube.

From Eqs. (2.6) and (2.7) the wave-vector components q_1 and q_2 can be expressed through the couple q and l and the equations of motion and the dynamical matrix can be written as

$$\omega^2(ql) e_\alpha(k|ql) = \sum_{k'\beta} D_{\alpha\beta}(kk'|ql) e_\beta(k'|ql) \quad (2.8)$$

and

$$D_{\alpha\beta}(kk'|ql) = \frac{1}{\sqrt{m_k m_{k'}}} \sum_{l'\delta} \Phi_{\alpha\delta}(\mathbf{0}k, l'k') S_{\delta\beta}(l') \times \exp[i(\alpha(l')l + z(l')q)]. \quad (2.9)$$

Here, $\alpha(l) = 2\pi(l_1 N_2 - l_2 N_1)/N_c$ and $z(l) = (L_1 l_2 - L_2 l_1)/N_c$ are the dimensionless coordinates of the origin of the l th cell along the circumference and along the tube axis, respectively. The equations of motion (2.8) yield the eigenvalues $\omega(qlj)$ and the corresponding eigenvectors $e_\alpha(k|qlj)$ where the couple (lj) ($l=0, \dots, N_c-1; j=1, \dots, 6$) labels the modes with a given wave number q in the one-dimensional Brillouin zone ($-\pi \leq q \leq \pi$). It can be easily proven that three translational and one rotational sum rules are fulfilled identically for this lattice-dynamical model giving rise to four acoustic branches without any additional corrections either to the dynamical matrix,²³ or to the force constants²⁴ (see Appendix A).

In some cases, it is important to know the eigenvectors and the dynamical matrix for the translational unit cell. The derivation of these quantities in terms of those for the two atoms unit cell is straightforward and eventually the following equations are obtained

$$e_\alpha(lk|qlj) = \sum_{\beta} S_{\alpha\beta}(l) e_\beta(k|qlj) \exp\{i[\alpha(l)l + z(l)q]\} \quad (2.10)$$

and

$$D_{\alpha\beta}(lk, l'k'|q) = \frac{1}{N_c} \sum_{l'\gamma\delta} S_{\alpha\gamma}(l) D_{\gamma\delta}(kk'|ql) S_{\delta\beta}(-l') \times \exp\{-i[\alpha(l')l + z(l')q]\}. \quad (2.11)$$

Here, the index l labels the two atoms unit cells within the translational unit cell, $\alpha(l') = \alpha(l') - \alpha(l)$ and $z(l') = z(l') - z(l)$. It is important to point out that the necessary computational time for solving the eigenvalue problem for the two atoms unit cell and subsequent use of Eq. (2.10) is nearly independent of the number of atoms in the translational unit cell. However, if the dynamical matrix is calculated from Eq. (2.11), this will require a time increasing as N_c^3 , which may be practically impossible for certain experimentally observable chiral SWNT's with large N_c .

B. Sound waves velocities and elastic moduli

Analytical expressions for the velocity of the sound waves in SWNT can be derived by studying the long-wavelength vibrational waves using Born's perturbation technique¹⁶ within the lattice-dynamical model developed above. Namely, the dynamical matrix Eq. (2.11) and the eigenvectors Eq. (2.10) and the eigenvalues belonging to the acoustic branches are expanded in power series in q . These expansions, substituted in the equations of motion for the translational unit cell, give rise to equations of zeroth, first, and second order with respect to the perturbation parameter q .

Taking nontrivial solutions for the zeroth-order eigenvector of the form

$$e_{\alpha}^{(0)}(\mathbf{l}k) = \sqrt{m_k} u_{\alpha} \quad (2.12)$$

with \mathbf{u} - a constant vector, and solving the zeroth-, first-, and second-order equations as in Ref.16 we obtain the system of linear equations for u_{α}

$$\rho v^2 u_{\alpha} = \sum_{\beta} \Lambda_{\alpha\beta} u_{\beta}. \quad (2.13)$$

Here, $\rho = N_c \sum_k m_k / V$ is the mass density of the tube, V is a (yet unspecified) ‘unit cell volume,’ and $v = \omega^{(1)}/q$ is the phase sound velocity. The matrix elements $\Lambda_{\alpha\beta}$ are defined by

$$\begin{aligned} \Lambda_{\alpha\beta} = & \frac{1}{V} \left[\sum_{\mathbf{l}k\mathbf{l}'k'} \sqrt{m_k m_{k'}} D_{\alpha\beta}^{(2)}(\mathbf{l}k, \mathbf{l}'k') \right. \\ & - \sum_{\mathbf{l}k\mathbf{l}'k'} \sum_{\mu\nu} \Gamma_{\mu\nu}(\mathbf{l}k, \mathbf{l}'k') \sum_{\mathbf{l}''k''} \sqrt{m_{k''}} D_{\mu\alpha}^{(1)}(\mathbf{l}k, \mathbf{l}''k'') \\ & \left. \times \sum_{\mathbf{l}'''k'''} \sqrt{m_{k'''}} D_{\nu\beta}^{(1)}(\mathbf{l}'k', \mathbf{l}'''k''') \right]. \quad (2.14) \end{aligned}$$

The matrices $D_{\alpha\beta}^{(1)}(\mathbf{l}k, \mathbf{l}'k')$ and $D_{\alpha\beta}^{(2)}(\mathbf{l}k, \mathbf{l}'k')$ are the first- and second-order dynamical matrices and the matrix $\Gamma_{\alpha\beta}(\mathbf{l}k, \mathbf{l}'k')$ is defined at the end of this section.

Equation (2.13) have nontrivial solutions only for certain values of v that are the sound velocity of the longitudinal wave v_L and the sound velocity of the transverse waves v_T

$$v_L = \sqrt{\frac{\Lambda_1}{\rho}}, \quad v_T = \sqrt{\frac{\Lambda_{2,3}}{\rho}}, \quad (2.15)$$

where $\Lambda_{\alpha} (\alpha=1,2,3)$ are the eigenvalues of the matrix $\Lambda_{\alpha\beta}$.

Besides the nontrivial solutions given in Eq. (2.12), the zeroth-order equations have also a nontrivial solution of the form

$$e_{\alpha}^{(0)}(\mathbf{l}k) = \sum_{\nu} \sqrt{m_k} \varepsilon_{\alpha\nu z} \theta_z R_{\nu}(\mathbf{l}k), \quad (2.16)$$

where without loss of generality we have chosen the z axis along the tube axis and, consequently, $\alpha=x,y$; $\varepsilon_{\alpha\beta\gamma}$ is the Levi-Civita symbol, θ_z is an angle of rotation about the z axis. Proceeding as in Ref. 16, we obtain the equation

$$\rho v^2 = \Lambda, \quad (2.17)$$

where

$$\begin{aligned} \Lambda = & \frac{1}{V} \left\{ \sum_{\alpha,\beta=x,y} \left[\sum_{\mathbf{l}k\mathbf{l}'k'} \sum_{\gamma\delta} \sqrt{m_k m_{k'}} D_{\alpha\beta}^{(2)}(\mathbf{l}k, \mathbf{l}'k') \varepsilon_{\alpha z \gamma} \right. \right. \\ & \times R_{\gamma}(\mathbf{l}k) \varepsilon_{\beta z \delta} R_{\delta}(\mathbf{l}'k') \\ & - \sum_{\mathbf{l}k\mathbf{l}'k'} \sum_{\mu,\nu} \Gamma_{\mu\nu}(\mathbf{l}k, \mathbf{l}'k') \sum_{\mathbf{l}''k''} \sqrt{m_{k''}} D_{\mu\alpha}^{(1)}(\mathbf{l}k, \mathbf{l}''k'') \varepsilon_{\alpha z \gamma} \\ & \left. \left. \times R_{\gamma}(\mathbf{l}''k'') \sum_{\mathbf{l}'''k'''} \sqrt{m_{k'''}} D_{\nu\beta}^{(1)}(\mathbf{l}'k', \mathbf{l}'''k''') \varepsilon_{\beta z \delta} R_{\delta}(\mathbf{l}'''k''') \right] \right\}. \quad (2.18) \end{aligned}$$

The sound velocity of the torsional wave in the tube, v_R , can be determined from Eq. (2.17) as

$$v_R = \sqrt{\frac{\Lambda}{\rho}}. \quad (2.19)$$

In Eqs. (2.14) and (2.18) the matrix $\Gamma_{\alpha\beta}(\mathbf{l}k, \mathbf{l}'k')$ is the inverse of the zeroth-order dynamical matrix $D_{\alpha\beta}^{(0)}(\mathbf{l}k, \mathbf{l}'k')$. However, this inversion cannot be done directly because of the linear dependence of elements of the latter. To carry out the inversion, we, following Born,¹⁶ remove one row and one column of $D_{\alpha\beta}^{(0)}(\mathbf{l}k, \mathbf{l}'k')$ for each α and β , remove one row and one column from its xy submatrix, invert the resulting matrix, and add rows and columns of zeros on the places of the removed ones.

The microscopically derived sound waves velocities Eqs. (2.15) and (2.19) can be used to derive the Young's modulus Y and the shear modulus G of the nanotube. For this purpose, we assume that a nanotube can be considered as an infinitely thin homogeneous cylinder with radius R and use the formulas from the theory of elasticity²⁵

$$v_L = \sqrt{\frac{Y}{\rho}}, \quad (2.20)$$

$$v_R = \sqrt{\frac{G}{\rho}}, \quad (2.21)$$

$$v_T^G = \sqrt{\frac{2Y}{\rho}} R q = \sqrt{2} R v_L q. \quad (2.22)$$

Comparing Eqs. (2.15) and (2.19) to Eqs. (2.20), (2.21), and (2.22), we identify Λ_1 and Λ as the Young's and the shear moduli of the tube, respectively, and find that $\Lambda_{2,3}$ must be zero. The Young's modulus can be determined alternatively from Eq. (2.22) and the transverse acoustic branches of the phonon dispersion curves.

III. RESULTS AND DISCUSSION

The lattice-dynamical model and the analytical expressions for the sound velocities can be applied now to calculate the phonon dispersion, Young's and shear moduli of various SWNT's. Since in a force-constant model of the lattice dynamics it is not possible to accomplish a real structural optimization, the structural data for the nanotubes has to be provided from the experiment or from theoretical estimations. The experimental data on the nanotube structure are rather scarce but two recent *ab initio* studies^{15,26} reveal that there are only slight differences between the various carbon-

carbon bond lengths and between the various bond angles. In accord with these results, we have chosen the simplest structural model accepting that for a given tube (1) all bond lengths are equal to 1.42 Å, the same as those in the graphene sheet, (2) all bond angles are equal to each other for a given tube, and (3) all atoms lie on a cylindrical surface. These assumptions are justified by the results of our preliminary calculations showing that deviations of the bond lengths and bond angles up to a few per cent from their values following from (1)–(3) and small departures from the ideal cylindrical geometry do not affect significantly the eigenmodes and the elastic moduli.

The lattice-dynamical model implements force constants of valence force field (VFF) type with values obtained by fitting to the surface phonon dispersion curves of graphite investigated by high-resolution electron energy-loss spectroscopy.¹⁸ The VFF parameters are of types nearest-neighbor stretch, next-to-nearest-neighbor stretch, in-plane bend, out-of-plane bend and twist interactions. Here, we additionally assume that these model parameters can be transferred to nanotubes without any modification. Nevertheless, effects due to the curvature of the tubes will still exist because the bond angles enter the force-constant matrix explicitly.

The calculated phonon dispersion of a (10,10) tube in Fig. 1 shows the presence of four acoustic branches—longitudinal, torsional, and a doubly degenerate transverse one. The former two increase linearly with the wave number and the latter one increases as the square of the wave number near the origin in agreement with the long-wavelength results presented above. To our knowledge, up to now there have been only a few calculations of the phonon dispersion in nanotubes. They have been accomplished either by the zone-folding method with a correction of the dynamical matrix in order to obtain the two transverse acoustic branches,²³ or by a simple force-constant model with modification of the force constants in order to fulfill the rotational sum rule and to obtain the torsional acoustic branch.²⁴ In the latter work it is obtained, however, that all the four acoustic modes have nonzero slopes at the origin. Recently, *ab initio* phonon dispersions for (4,4) and (10,10) tubes that are free from the zone-folding model deficiencies have been published.¹⁵ However, these *ab initio* results predict frequencies for the highest zone-center phonons that are about 6% higher than the experimental values and in this respect they cannot compete with the simple force-constant models.

The estimation of the elastic moduli of nanotubes requires the knowledge of the “unit cell volume” V of the tubes. There is no agreement between the different authors about the choice of the continuum model of a nanotube. Some of them consider a nanotube as a hollow cylinder with a certain wall thickness, e.g., 0.66 Å (Ref. 12) or 3.4 Å (Ref. 10)—equal to the adjacent layer separation in graphite. Others choose a uniform cylinder with a cross-sectional area of πR^2 (Ref. 13) or a prism—the unit cell in a crystalline rope of SWNT's,⁴ with a cross-sectional area of $\sqrt{3}/2(2R+3.4)^2$ (Ref. 9). Recently, it was proposed to characterize the axial stiffness of a nanotube with the second derivative of the strain energy with respect to the axial strain per unit area of the nanotube¹⁴ or per atom of the tube.¹⁵ In the latter case, the resulting quantity is equal to the Young's modulus multiplied by the tube volume per atom v_a so that it does not

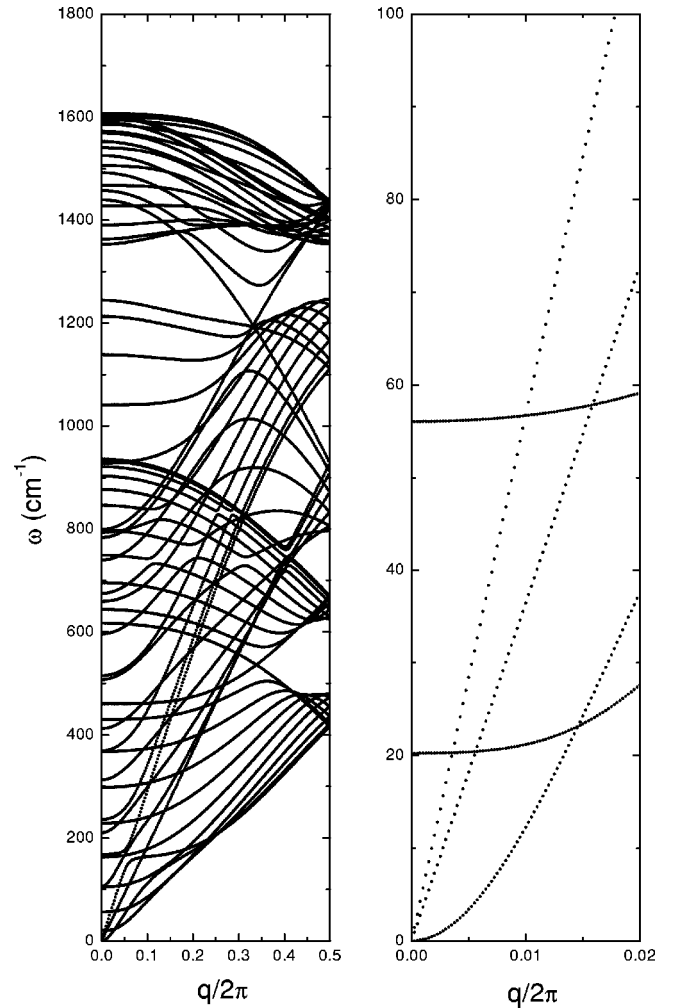


FIG. 1. Calculated phonon dispersion curves for a (10,10) SWNT (left) and the low-energy region of the same curves containing the translational, the torsional and the doubly degenerate transverse acoustic branches (right).

contain the ambiguous unit-cell volume. For this reason, we adopt such a description of the elastic properties of the tubes for both axial and shear strains.

The in-plane elastic moduli, calculated for graphene with the adopted VFF parameters, are compared to the corresponding experimental values for graphite in Table I. The agreement between these values is quite good and it may be expected that these VFF parameters would allow for fair predictions of the elastic moduli of nanotubes as well. The Young's and shear moduli of SWNT's are calculated here using Eqs. (2.14) and (2.18) for various tube types: armchair tubes from (3,3) to (15,15), zigzag tubes from (5,0) to (25,0), and a number of chiral tubes [(5,1), (5,2), (6,1), (5,3), (6,2), (7,1), (6,3), (6,4), (8,2), (7,4), (10,1), (8,4), (9,3), (8,5), (11,2), (10,4), (10,5), (12,3), (14,2), (12,6), (16,4), (14,7), and (15,6)—in order of increasing tube radius]. The results for the moduli and the Poisson ratio vs tube radius are displayed in Fig. 2. We note that Y can be determined alternatively from the transverse acoustic branches of the dispersion curves fitted with a polynomial of second degree with respect to the wave number and the expression for the group sound velocity of the bending waves (2.22) leading to the same results as those obtained by using Eqs. (2.15) and (2.20). The

TABLE I. Experimental elastic constants (in GPa) and elastic moduli (in GPa/in eV) and Poisson ratio for graphite in comparison with the calculated ones here.

| | c_{11} | c_{12} | c_{66}^a | Y^b | G^b | ν^b |
|------------------------------|----------|----------|------------|------------|-----------|---------|
| Experim. values ^c | 1060 | 180 | 440 | 1029/56.43 | 440/24.13 | 0.17 |
| Calc. values (this work) | 1047 | 219 | 414 | 1002/54.95 | 414/22.70 | 0.21 |

^aFor hexagonal symmetry, $c_{66} = (c_{11} - c_{12})/2$.

^bIn-plane moduli $Y = (c_{11}^2 - c_{12}^2)/c_{11}$ and $G = c_{66}$, and Poisson ratio $\nu = c_{12}/c_{11}$.

^cRef. 27.

results for Y , presented in Fig. 2, show that for a given radius the Young's modulus for armchair tubes is slightly larger than for zigzag tubes and that for chiral tubes it has intermediate values. As a whole, the Young's modulus is insensitive to the tube chirality and for large radii has values of about 55 eV that are about 3% smaller than the experimental one for graphite (see Table I). At small radii the Young's modulus softens to about 50 eV. The first MD simulations¹² predict for the Young's modulus of a (10,10) tube the value 59.4 eV which differs only by a few percent from our results. However, the calculations within another MD simulations scheme¹³ and with a TB model¹⁴ yield for Y values of about 35 eV and about 70 eV, respectively, that significantly underestimate and overestimate Young's modulus of a tube. Recently, pseudopotential DFT calculations¹⁵ of several SWNT's resulted in average Young's modulus of 56 eV. The only available experimental point⁷ is nearer to the TB (Ref. 14) and the DFT results¹⁵ for the same tube radius but the

force-constant results¹⁰ as well as ours are also within the range of the experimental error of the former.

The shear modulus behaves similarly to the Young's modulus reaching values of about 23 eV for large radii but softening at small radii as shown in Fig. 2. The direct comparison of the obtained results with the experimental data for graphite (see Table I) reveals systematic deviation of about 6% for the shear modulus at large radii, which we attribute to the VFF parameters of the model and to the initial assumptions. The shear moduli calculated for several tube types within a force-constant model¹⁰ appear to be insensitive to the tube radius and chirality and are about 15% higher than the ones obtained here.

Using Y and G , we can estimate the Poisson ratio ν , that is equal to the ratio of the relative radial tube expansion to the relative axial tube shortening, making use of the expression valid for a three-dimensional isotropic medium:⁶ $\nu = (Y/2 - G)/G$. The spread in the values of both moduli has as a consequence a spread in the values of the Poisson ratio that is more prominent for small tube radii (see the inset in Fig. 2). In the limit of large radii, the Poisson ratio tends to 0.21 that is close to the experimental value for graphite (see Table I). The Poisson ratio estimated by means of a force-constant model¹⁰ is practically a constant of 0.28 that is about 1.6 times larger than the in-plane value for graphite. A possible reason for this disagreement may be that the chosen model cannot describe properly the energy of radially strained tubes. The same behavior has TB results¹⁴ that range from 0.247 to 0.275. The recently calculated Poisson ratio by a DFT model¹⁵ varies from 0.12 to 0.19 for a number of tube types and for large tube radii has values that are close to the experimental value for graphite.

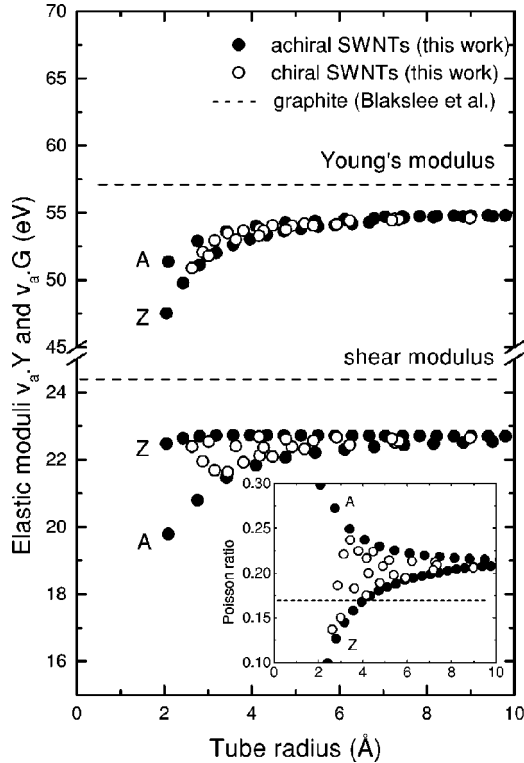


FIG. 2. Calculated Young's and shear moduli times the volume per atom of the tube v_a (in eV), and Poisson ratio estimated using the relation $\nu = (Y/2 - G)/G$ (in the inset) vs tube radius for various chiral and achiral SWNT's. The notations A and Z stand for "armchair" and "zigzag," respectively.

IV. CONCLUSIONS

In this paper, Young's and shear moduli of various SWNT's are estimated from analytical formulas derived within a lattice-dynamical model for nanotubes. The results for the elastic moduli and Poisson ratio obtained here using force constants of the VFF type are in fair agreement with the existing experimental data on graphite and nanotubes. These results compare well to the best results of more refined models—potential-based molecular-dynamics, tight-binding and DFT models. The force-constant model has the essential advantage to the latter models that it has a low-computational cost with respect to both computer memory and processing time. In particular, the use of analytical formulas allows one to obtain the elastic moduli of a given tube in one calculational step only. Due to the large values of the

Young's modulus along the tube's axis, the SWNT's are one of the stiffest materials. This property, combined with their relatively small mass density, makes them ideal ingredients for composites.

ACKNOWLEDGMENTS

This work was supported partly by Grant No. G.0347.97 of the Flemish Science Foundation and partly by the Concerted Action of the University of Antwerp GOA-BOF-UA Nr.23. Two of us (V. E. V. D. and V. N. P.) acknowledge the financial support from the Scientific Affairs Division of NATO under Grant No. CRG 973953.

APPENDIX A: TRANSLATIONAL AND ROTATIONAL SUM RULES

The infinitesimal translational and rotational invariance conditions impose constraints on the force constants. If the undistorted crystal is translated by an infinitesimal vector ε_β , this will not give any contribution to the restoring force in Eq. (2.2), i.e.,

$$0 = \sum_{l'k'\beta} \Phi_{\alpha\beta}(\mathbf{l}k, \mathbf{l}'k') \varepsilon_\beta. \quad (\text{A1})$$

This equation can be transformed in the form

$$0 = \sum_{\gamma\delta\beta} S_{\alpha\gamma}(\mathbf{l}) \left[\sum_{l'k'} \Phi_{\gamma\delta}(\mathbf{0}k, \mathbf{l}'k') \right] S_{\delta\beta}(-\mathbf{l}) \varepsilon_\beta. \quad (\text{A2})$$

Since the rhs of Eq. (A2) is zero for arbitrary \mathbf{l} and ε_β , we may set $\mathbf{l} = \mathbf{0}$ and obtain the translational sum rule as

$$0 = \sum_{l'k'} \Phi_{\alpha\beta}(\mathbf{0}k, \mathbf{l}'k'). \quad (\text{A3})$$

Equation (A3) enables the determination of the "self" force constant

$$\Phi_{\alpha\beta}(\mathbf{0}k, \mathbf{0}k) = - \sum_{l'k' (l'k' \neq \mathbf{0}k)} \Phi_{\alpha\beta}(\mathbf{0}k, \mathbf{l}'k'). \quad (\text{A4})$$

An infinitesimal rotation performed on the undistorted crystal results in the atomic displacements

$$u_\alpha(\mathbf{l}k) = \sum_{\beta\mu\nu} S_{\alpha\beta}(\mathbf{l}) \varepsilon_{\beta\mu\nu} \theta_\mu R_\nu(k), \quad (\text{A5})$$

where θ_α is an infinitesimal rotation angle about the α axis. Such a rotation gives no contribution to the restoring force in Eq. (2.2), i.e.,

$$0 = \sum_{l'k' \gamma\beta\mu\nu} \Phi_{\alpha\gamma}(\mathbf{l}k, \mathbf{l}'k') S_{\gamma\beta}(\mathbf{l}') \varepsilon_{\beta\mu\nu} \theta_\mu R_\nu(k'). \quad (\text{A6})$$

Here, $\varepsilon_{\beta\mu\nu}$ is the Levi-Civita tensor. The rhs of Eq. (A6) can be written as

$$0 = \sum_{\gamma\mu} S_{\alpha\gamma}(\mathbf{l}) \left[\sum_{l'k' \delta\beta\nu} \Phi_{\gamma\delta}(\mathbf{0}k, \mathbf{l}'k') \right. \\ \left. \times S_{\delta\beta}(\mathbf{l}'-\mathbf{l}) \varepsilon_{\beta\mu\nu} R_\nu(k') \right] \theta_\mu. \quad (\text{A7})$$

Since the rhs of Eq. (A7) is zero for arbitrary \mathbf{l} and θ_μ , the rotational sum rule is obtained eventually as

$$0 = \sum_{l'k' \delta\beta\mu\nu} \Phi_{\alpha\delta}(\mathbf{0}k, \mathbf{l}'k') S_{\delta\beta}(\mathbf{l}') \varepsilon_{\beta\mu\nu} R_\nu(k'). \quad (\text{A8})$$

Consider now the case $\mathbf{q} \rightarrow \mathbf{0}$. If we assume a solution to Eq. (2.4) in the form

$$e_\alpha(k|\mathbf{0}) = \sqrt{m_k} \varepsilon_\alpha, \quad (\text{A9})$$

we get

$$\omega^2(\mathbf{0}) \varepsilon_\alpha = \sum_{\delta\beta} \left[\sum_{l'k'} \Phi_{\alpha\delta}(\mathbf{0}k, \mathbf{l}'k') \right] S_{\delta\beta}(\mathbf{l}') \varepsilon_\beta. \quad (\text{A10})$$

The rhs of Eq. (A10) vanishes due to the translational sum rule (A3) and this gives rise to three acoustical modes with $\omega(\mathbf{0}) = 0$.

Let us assume the solution

$$e_\alpha(k|\mathbf{0}) = \sum_{\mu\nu} \sqrt{m_k} \varepsilon_{\alpha\mu\nu} \theta_\mu R_\nu(k). \quad (\text{A11})$$

Then Eq. (2.4) becomes

$$\omega^2(\mathbf{0}) \sum_{\mu\nu} \varepsilon_{\alpha\mu\nu} \theta_\mu R_\nu(k) \\ = \sum_{\mu} \left[\sum_{l'k' \delta\beta\nu} \Phi_{\alpha\delta}(\mathbf{0}k, \mathbf{l}'k') S_{\delta\beta}(\mathbf{l}') \varepsilon_{\beta\mu\nu} R_\nu(k') \right] \theta_\mu. \quad (\text{A12})$$

The rhs of Eq. (A12) vanishes in view of the rotational sum rule (A8) and we get $\omega(\mathbf{0}) = 0$. However, from here, the existence of only one torsional acoustic mode follows because of the restriction for small atomic displacements.

*Permanent address: Faculty of Physics, University of Sofia, BG-1164 Sofia, Bulgaria.

¹S. Iijima, *Nature* (London) **354**, 56 (1991).

²S. Iijima and T. Ichihashi, *Nature* (London) **363**, 603 (1993); D.S. Bethune, C.-H. Kiang, M.S. de Vries, G. Gorman, R. Savoy, J. Vasquez, and R. Beyers, *ibid.* **363**, 605 (1993).

³M. S. Dresselhaus, G. Dresselhaus, and P. C. Eklund, *Science of*

Fullerenes and Carbon Nanotubes (Academic, New York, 1996).

⁴A. Thess, R. Lee, P. Nikolaev, H. Dai, P. Petit, J. Robert, C. Xu, Y.H. Lee, S.G. Kim, A.G. Rinzler, D.T. Colbert, G.E. Scuseria, D. Tománek, J.E. Fischer, and R.E. Smalley, *Science* **273**, 483 (1996).

⁵C. Journet, W.K. Maser, P. Bernier, A. Loiseau, M. Lamy de la

- Chapelle, S. Lefrant, P. Deniard, R. Lee, and J.E. Fischer, *Nature* (London) **388**, 756 (1997).
- ⁶M.M.J. Treacy, T.W. Ebbesen, and J.M. Gilson, *Nature* (London) **381**, 678 (1996).
- ⁷A. Krishnan, E. Dujardin, T.W. Ebbesen, P.N. Yianilos, and M.M.J. Treacy, *Phys. Rev. B* **58**, 14 013 (1998).
- ⁸E.W. Wong, P.E. Sheehan, and C.M. Lieber, *Science* **277**, 1971 (1997).
- ⁹J.-P. Salvetat, G.A.D. Briggs, J.-M. Bonard, R.R. Bacsá, A.J. Kulik, T. Stöckli, N.A. Burnham, and L. Forró, *Phys. Rev. Lett.* **82**, 944 (1999).
- ¹⁰J.P. Lu, *Phys. Rev. Lett.* **79**, 1297 (1997).
- ¹¹D.H. Robertson, D.W. Brenner, and J.W. Mintmire, *Phys. Rev. B* **45**, 12 592 (1992).
- ¹²B.I. Yakobson, C.J. Brabec, and J. Bernholc, *Phys. Rev. Lett.* **76**, 2511 (1996).
- ¹³C.F. Cornwell and L.T. Wille, *Solid State Commun.* **101**, 555 (1997).
- ¹⁴E. Hernández, C. Goze, P. Bernier, and A. Rubio, *Phys. Rev. Lett.* **80**, 4502 (1998).
- ¹⁵D. Sánchez-Portal, E. Artacho, J.M. Soler, A. Rubio, and P. Ordejón, *Phys. Rev. B* **59**, 12 678 (1999).
- ¹⁶M. Born and K. Huang, *Dynamical Theory of the Crystal Lattices* (Oxford University Press, Oxford, 1954).
- ¹⁷V.N. Popov, V.E. van Doren, and M. Balkanski, *Phys. Rev. B* **59**, 8355 (1999).
- ¹⁸T. Aizawa, R. Souda, S. Otani, Y. Ishizawa, and C. Oshima, *Phys. Rev. B* **42**, 11 469 (1990); **43**, 12 060(E) (1991).
- ¹⁹N. Hamada, S.-I. Sawada, A. Oshiyama, *Phys. Rev. Lett.* **68**, 1579 (1992).
- ²⁰R. Saito, M. Fujita, G. Dresselhaus, and M.S. Dresselhaus, *Phys. Rev. B* **46**, 1804 (1992).
- ²¹C.T. White, D.H. Robertson, and J.W. Mintmire, *Phys. Rev. B* **47**, 5485 (1993).
- ²²R.A. Jishi, M.S. Dresselhaus, and G. Dresselhaus, *Phys. Rev. B* **47**, 16 671 (1993).
- ²³R.A. Jishi, L. Venkataraman, M.S. Dresselhaus, and G. Dresselhaus, *Chem. Phys. Lett.* **209**, 77 (1993).
- ²⁴R. Saito, T. Takeya, T. Kimura, G. Dresselhaus, and M.S. Dresselhaus, *Phys. Rev. B* **57**, 4145 (1998).
- ²⁵L. D. Landau and E. M. Lifshitz, *Theory of Elasticity* (Pergamon, Oxford, 1995).
- ²⁶J. Kürti, G. Kresse, and H. Kuzmany, *Phys. Rev. B* **58**, R8869 (1998).
- ²⁷O.L. Blakslee, D.G. Proctor, E.J. Seldin, G.B. Spence, and T. Weng, *J. Appl. Phys.* **41**, 3373 (1970).